UCRL-2100

UNCLASSIFIED

UNIVERSITY OF CALIFORNIA — BERKELEY

TWO-WEEK LOAN COPY

This is a Library Circulating Copy which may be borrowed for two weeks. For a personal retention copy, call Tech. Info. Division, Ext. 5545

RADIATION LABORATORY

DISCLAIMER

This document was prepared as an account of work sponsored by the United States Government. While this document is believed to contain correct information, neither the United States Government nor any agency thereof, nor the Regents of the University of California, nor any of their employees, makes any warranty, express or implied, or assumes any legal responsibility for the accuracy, completeness, or usefulness of any information, apparatus, product, or process disclosed, or represents that its use would not infringe privately owned rights. Reference herein to any specific commercial product, process, or service by its trade name, trademark, manufacturer, or otherwise, does not necessarily constitute or imply its endorsement, recommendation, or favoring by the United States Government or any agency thereof, or the Regents of the University of California. The views and opinions of authors expressed herein do not necessarily state or reflect those of the United States Government or any agency thereof or the Regents of the University of California.

UCRL-2102

UNIVERSITY OF CALIFORNIA

Radiation Laboratory

Contract No. W-7405-eng-48

THE PRODUCTION OF POSITIVE PIONS BY 341 MEV PROTONS ON PROTONS

W. F. Cartwright, C. Richman, M. N. Whitehead, and H. A. Wilcox

March 18, 1953

Berkeley, California

THE PRODUCTION OF POSITIVE PIONS BY 341 MEV PROTONS ON PROTONS*

W. F. Cartwright,** C. Richman, M. N. Whitehead and H. A. Wilcox***

Radiation Laboratory, Department of Physics,
University of California, Berkeley, California

March 18, 1953

ABSTRACT

The production of positive pions by protons on protons has been studied at 0°, 35° and 58° to the beam of 341 Mev protons produced by the Berkeley synchro-cyclotron. In the collision of two protons, two reactions are possible which lead to a π^+-meson: (1) $P + P \rightarrow \pi^+ + D$ and (2) $P + P \rightarrow \pi^+ + N + P$. The experimental results at 0° show an energy spectrum from 0 to 70 Mev which is farily flat except for a large peak at the high energy end. The flat portion of the spectrum can only be due to reaction (2). A comparison of the shape of the peak with the results of the phenomenological theory of Brueckner and Watson shows that the peak is due solely to reaction (1).

This fact, together with a measurement of the energy of the beam and of the energy of the pions from reaction (1), gives the value 275.1±2.5 electron masses for the mass of the positive pion. The angular distribution in the center of mass system for reaction (1) as obtained from the data at the above three angles, is $3.3 \pm 1.2 \left[.11 \pm .06 + \cos^2\theta \right] \cdot 10^{-29} cm^2$ st erad.$^{-1}$ and the total cross section for reaction (1) is $1.8 \pm 0.6 \cdot 10^{-28} cm^2$.

These results have been compared with the results obtained by Durbin, Loar, and Steinberger and by Clark, Roberts, and Wilson on the inverse reaction, $\pi^+ + D \rightarrow P + P$. Using the theorem of detailed balancing, these experiments lead to the value zero for the spin of the positive pion with good certainty.

---

* Preliminary results of this experiment were given in Phys. Rev. 78, 823 (1950), Phys. Rev. 79, 85 (A) (1950), Phys. Rev. 82, 460 (1951), and Phys. Rev. 83, 855 (1951).

** Now at the University of Rochester, Rochester, N. Y.

*** Now at the Naval Ordnance Test Station, China Lake, California.

THE PRODUCTION OF POSITIVE PIONS BY 341 MEV PROTONS ON PROTONS

W. F. Cartwright, C. Richman, M. N. Whitehead and H. A. Wilcox

Radiation Laboratory, Department of Physics,
University of California, Berkeley, California

March 18, 1953

I. INTRODUCTION

The early investigations of the cross sections for the production of pions by 341 Mev protons, undertaken at the Berkeley 184-inch synchrocyclotron, were made by bombarding various complex nuclei.[1, 2]

It is expected that the analysis of the pion production process should be much more incisive for the case of a simple nucleon-nucleon collision than for the earlier experiments. An experiment was therefore undertaken to measure the yield of positive pions produced by 341 Mev protons on hydrogen.

Since the proton beam energy is about 50 Mev above the threshold for the production of pions in this process, $P + P \rightarrow \pi^+$, the pion velocity in the center of mass system is comparable to the velocity of the center of mass relative to the laboratory system. Consequently, the pions are emitted primarily in the forward direction in the laboratory; that is, in the direction of the proton beam. It was found possible, by using a magnetic field, to separate the pions produced in the forward direction from the proton beam, and an investigation was made of the energy spectrum of the pions produced at zero degrees.

The initial experiments[3] showed an energy spectrum that was fairly flat except for a large peak at the high energy end. There are two possible reactions in which the pions may be produced, namely:

$$P + P \rightarrow \pi^+ + D \qquad (1)$$

$$P + P \rightarrow \pi^+ + N + P. \qquad (2)$$

It was suggested[4] that the first reaction is primarily responsible for the peak at the end of the spectrum. A careful measurement was then made of the shape of the spectrum near the maximum energy in order to determine whether this was the case.

Later measurements were also made of the yield of pions at 35° and 58° to the proton beam in order to determine the angular distribution of the pions in the center of mass system.

It was pointed out by Johnson,[5] and independently by Marshak[6] and Cheston,[7] that the principle of detailed balance can be applied to reaction (1) and its inverse to obtain the spin of the positive pion. A knowledge of the angular distribution of (1) makes possible the detailed comparison of this experiment with the experiments on the inverse reaction.

II. GENERAL METHOD

For this experiment the electrically deflected 341 Mev proton beam of the Berkeley synchro-cyclotron was used. The method of deflection and collimation of the beam have been described previously.[7]

The method used for studying the production from hydrogen is an extension of that developed for measuring the cross section for the production of mesons by protons on heavy nuclei at 90° to the proton beam.[8] It has been modified by the use of a channel and magnetic field to decrease the background of scattered protons which caused difficulty in those experiments.

Figure 1 shows a schematic diagram of the experimental set-up. The collimated proton beam passes through an ionization chamber and then strikes either a graphite or polyethylene target which is placed between the pole faces of the magnet.

The pions bend away from the proton beam and those in the energy interval and angular interval of interest pass through the wide channel cut in the brass shielding and enter the absorber-detector. They are slowed down by ionization in the absorber and the population of stopped pions is sampled by a nuclear emulsion embedded in the absorber. The developed plate is scanned and the positive pions identified by the nature of the pion track and by the characteristic μ decay track at the end of the range.

The success of this method depends on the fact that a pion with the same momentum as a proton has, as a consequence of the large mass difference, a range approximately one hundred times that of the proton. The protons coming down the channel are therefore stopped in the first part of the absorber and are eliminated as a source of background in the scanned region of the emulsion.

The brass shielding which forms the channel serves only to protect the detector from high energy protons scattered from the target and to limit the angular spread at the target of the pions detected.

One can calculate the number of pions per square centimeter per Mev hitting the face of the absorber from the density of stopped pions in the emulsion. If the solid angle subtended at the target by a unit area at the absorber is known, the cross section can then be calculated in the usual manner.

The calibrated ion chamber placed before the target gives the total number of protons passing through it, making possible the calculation of absolute production cross sections.

Since this arrangement accepts pions produced with a small spread of angles and in a small energy interval, several runs are made to cover the entire energy spectrum at each particular angle.

III. ABSORBER AND DETECTOR

The position of the nuclear plate in the absorber and the type of absorber used are shown in Fig. 2. As can be seen in the figure, the position of a pion's decay in the plate is a measure of the pion's range in the absorber, and therefore of its initial energy upon entering the absorber.

The cross sectional dimensions of the absorber were made large compared to the mean lateral displacement of the pions due to the multiple Coulomb scattering suffered by them while slowing down. If the pions from the target strike all parts of the absorber face, a condition of "poor geometry" obtains and it may be assumed that as many pions scatter into that part of the beam which stops in the emulsion as scatter out of it.

The root mean square lateral displacement calculated for 70 Mev pions was approximately 8 mm. The width and height of the absorbers were always much larger than this.

The number of stopped pions was found by scanning the developed plates under the microscope using a 90x oil immersion objective and 6x eyepieces. The microscopes were equipped with a special stage which was designed and built by Mr. W. M. Brower of the Physics Department machine shop. This stage enables the observer to reset the microscope to an accuracy of about 2 microns and enables him to determine with good accuracy the area which has been scanned. The photographic plates used were Ilford Nuclear Research plates, type C-2 and type C-3, with an emulsion thickness of 200 microns.

An event was counted as a π-μ decay only if either the π or the μ track could be definitely identified as a meson by the usual tests of

scattering or of rapid grain density variation. It is estimated that with this procedure the error in the number of pions observed is less than 5 percent.

For the high energy pions near the peak in the 0° pion spectrum, a copper slab was placed in front of the aluminum absorber holding the emulsion. This is shown in Fig. 2B. With this arrangement, the pions rapidly lost most of their energy by traveling a short distance in the copper, and the energy spectrum was then spread out along the nuclear plate because of the low stopping power of the aluminum. The range-energy curves of Aron, Hoffman, and Williams,[9] as corrected by the recent work of Mather and Segre,[10] were used to convert the pion range to energy. These latest corrected curves are accurate to about 0.5 percent in energy.

The absorber face was cut so that the pions entered normally. Thus, the variation in depth of penetration with angle of incidence is very small. For the zero degree measurements, with a one inch diameter target, and with the maximum channel width used, this angle varied between $+3^{\circ}$ and, -3°, depending on the energy of the meson and on its points of origin and decay. This produced an uncertainty in depth of penetration of less than 0.2 percent.

In order to find the density of stopped pions, it is necessary to know the thickness of the emulsion before development. It was possible to calculate this value from the thickness of the processed emulsion determining the shrinkage factor using either the alpha particle calibration method of Wilcox,[8] or the similar method of Barkas[11] using x-rays.

IV. CHANNEL

The principal purposes of the channel are to shield the detector from other particles and to insure that the pions enter the detector normally. The energy of the pions is determined by their depth of penetration into the absorber-detector. The minimum width of the channel exit is fixed by the requirement of poor geometry discussed above. The rest of the channel is then designed to allow pions in the desired energy range to reach all points of the absorber face from each part of the target.

For the 0° production experiment the channel accepted a 20 Mev energy interval around the peak. At the other angles it was necessary to use several values of the magnetic field with the same channel in order to cover a comparable energy interval. In these cases the energy intervals in the different runs were made to overlap.

V. TARGETS

The high cross section of hydrogen in the neighborhood of the peak, relative to that of carbon, made the use of a subtraction method practical. By measuring the pion yield from both polyethylene, $(CH_2)_n$, and carbon, the hydrogen cross section may be calculated with good accuracy.

In the region of the high energy peak, targets of one-quarter inch thickness were used to obtain good energy resolution. For the slowly varying continuum from hydrogen, and for the carbon data at 0°, one-half inch targets were used to keep the cyclotron bombardment time within reasonable limits. The effective area of the target was that of the proton beam, which was collimated to a one-inch diameter circular area by a 40-inch tube in the cyclotron shielding. The target densities were calculated from the measured weights and volumes.

VI. MAGNETIC FIELD

The magnetic field used to separate the pions from the proton beam was produced by a magnet whose maximum field was about 14,000 gauss over an area sufficiently large to turn a 70 Mev pion trajectory through about 90 degrees. The gap between the pole faces was 3.5 inches. The proton nuclear induction resonance method was used to measure the field to an accuracy better than one percent. The variation of the field, in time, during any particular run, never exceeded one percent.

VII. BEAM INTEGRATION

The ions produced by the proton beam in the ion chamber were collected on a condenser and the total charge measured by a standard electronic integrating circuit. The ion chamber had previously been calibrated by comparison with the total charge obtained by stopping the proton beam in a Faraday cup. The average beam current was around 10^{-10} amperes. The overall accuracy of the charge measurement is estimated to be better than ±5 percent.

VIII. GEOMETRY

From the density of the pions in the emulsion one can obtain the flux of pions of a given energy in the absorber. In order to calculate the differential production cross section, it is necassary to know the solid angle subtended at a point in the target by a unit area in the absorber.

If the trajectories lie in a plane perpendicular to the uniform magnetic field, the solid angle subtended by a unit area perpendicular to the trajectories is,[12]

$$\frac{d\Omega}{dA} = \frac{1}{\rho^2 \phi \sin \phi} , \qquad (3)$$

where ρ is the radius of curvtture of the pion trajectory, and ϕ is the angle through which it turns from the target to the absorber. This formula applies, within 2 percent, even though the field departs from uniformity near the pole boundaries, where ρ remains the radius of curvature in the uniform portion of the field.

A small error is introduced by the use of this formula for pions whose trajectories have a small component along the direction of the magnetic field. For the dimensions used in this experiment, this error was less than 0.1 percent, so no corrections have been made. Also, the finite size of the target and absorber cause some variation in the solid angle ($\sim$7 percent) for pions of different points of origin and termination. The value of $d\Omega/dA$ which was used in the calculations was for a trajectory from the center of the target to the center of the absorber.

IX. CALCULATION OF THE CROSS SECTION

The number of pions in a given energy interval that entered the absorber can be deduced from the number of pions stopped in the emulsion by the following argument. We will make the simplifying approximation that the pions travel in straight lines.

Consider pions of a given energy, E, which enter the absorber normally to and over the entire area of the face of the absorber. Let these pions have a range in the absorber which is R_o. Those pions whose trajectories lie between two lines, M_1 and M_2, as shown in Fig. 3, will stop in the emulsion, while pions whose trajectories lie outside of these lines will stop only in the aluminum absorber. It is easy to see that the height, a, between the two trajectories is d sec α R_{ab}/R_{em}, where d is the thickness of the emulsion, α is the angle of inclination of the plate as shown in the figure, and R_{em} and R_{ab} are the residual ranges of a meson of residual energy, E_{res}, in emulsion and absorber respectively. For $\alpha = 15^\circ$ and d = 200μ, E_{res} = 5.7 Mev and R_{ab}/R_{em} = 1.20.

Let the number of pions entering the absorber per unit area in an energy interval ΔE be $N(E)\,\Delta E$. If then we scan a strip of emulsion of length ℓ, perpendicular to the plane of Fig. 3, the number of pions that have stopped in the emulsion will be $N(E)\Delta E \cdot a \cdot \ell$.

The spread in pion energies, ΔE, in the beam, corresponding to a distance ΔZ along the plate (in the plane of Fig. 3) is given by: $\Delta E = \Delta Z \cos \alpha \, (-dE/dx)_{ab}$ where $(-dE/dx)_{ab}$ is the rate of energy loss per cm in the absorber at the initial energy of the pions. Thus, the number of mesons that stop in the area $\Delta Z \cdot \ell$ on the plate is given by $n = N(E)\,(-dE/dx)_{ab} \cos \alpha \cdot a \cdot \ell \cdot \Delta Z$. If d denotes the thickness of the emulsion and q represents the number of stopped pions found per unit volume of the emulsion, we obtain:

$$N(E) = \frac{n}{\left(\frac{-dE}{dx}\right)_{ab}\left(\frac{R_{ab}}{R_{em}}\right)\ell \cdot d \cdot \Delta Z} = \frac{q}{\left(\frac{-dE}{dx}\right)_{ab}\frac{R_{ab}}{R_{em}}} \tag{5}$$

The number of pions of energy E per Mev per cm^2 in the beam is given by:

$$N(E) = \frac{d\sigma}{dE\,d\Omega}\; N_p \; \frac{t \cdot D}{A} \; A_o \; \frac{d\Omega}{dA} \tag{6}$$

where N_p is the total number of protons that have passed through the target, D is the density of the target material, A_o is Avagadro's number, A is the molecular weight of carbon (or CH_2), t is the target thickness, $d\sigma/(dE\,d\Omega)$ is the differential cross section for production of mesons by protons on a carbon nucleus (or a CH_2 molecule) per unit solid angle per Mev, and $d\Omega/dA$ is the solid angle per unit area in the emulsion.

Using eqs. (5) and (6), the differential cross section is therefore found to be as follows:

$$\frac{d\sigma}{dE\,d\Omega} = \frac{q}{\left(\frac{-dE}{dx}\Big|_{ab}\right)\frac{R_{ab}}{R_{em}} \; N_p \cdot D \cdot t \; \frac{A_o}{A} \cdot \frac{d\Omega}{dA}} \quad cm^2\ Mev^{-1}\ sterad.^{-1} \tag{7}$$

Three corrections have to be made to eq. (7). (a) Some of the pions decay in flight before reaching the emulsion. The mean life of the π^+-meson has been found to be $2.65 \pm 0.12 \times 10^{-8}$ sec.[13] If the meson moves a distance, dr, in the laboratory with a momentum p_π, the proper time interval that has elapsed is:

$$d\tau = M_\pi \, dr / (p_\pi C^2)$$

where M_π is the rest energy of the meson, and c is the velocity of light.

In computing the correction to eq. (7) due to decay in flight, we neglect energy loss in air, and use, for the absorber, the empirical range energy relation:[14]

$$T_\pi = K R^n \tag{8}$$

where $n = 0.58$, K is a constant of the absorber material, T_π is the meson's kinetic energy, and R is its range. It can then be shown that the cross section as calculated from eq. (7) should be multiplied by the factor

$$\text{Exp} \left\{ 0.63\, 10^{-3} \left[x + x^2\right]^{-1/2} \rho \phi + 0.89\, 10^{-3}\, x^{-1/2} R \right\} \tag{9}$$

where $x = T_\pi/(2 M_\pi)$. This formula is easily extended to the case of a composite absorber.

(b) The pions emerging from the target in a given energy interval, ΔE, are produced at different depths of the target in different energy intervals, $\Delta E'$. When this is averaged over the target, one finds that $(\Delta E/\Delta E') = (-dE/dx_2) \cdot t/(E_2 - E_1)$, where $-dE/dx_2$ is the specific ionization at the exit side of the target, $E_2 - E_1$ is the energy loss in the target of a pion created at the front face, and t is the target thickness. The pion spectra are plotted as originating from the center of the target znd the yields are increased by this factor.

(c) The observed number of pions is decreased from the actual number entering the absorber by large angle nuclear scattering and absorption in the copper and aluminum. A precise measurement of the cross sections for these processes as a function of pion energy is not available, but recent experiments[15] indicate that for the energies involved in our experiment the attenuation cross section is less than nuclear area. We have corrected our data using a total attenuation cross section of 0.8 nuclear area independent of the energy of the pion.

X. EXPERIMENTAL RESULTS

Tables I, II, and III give the cross sections obtained from CH_2 andC at $0^\circ \pm 3^\circ$, $35^\circ \pm 3^\circ$, and $58^\circ \pm 3^\circ$ in the laboratory. The energies given are the production energies of the pions as deduced from the thicknesses of the target, air and abosrber traversed. The experimental cross sections, the corrections discussed above, and the final corrected values are listed. The errors shown are the statistical probable errors calculated from the

number of pions counted at each energy. The hydrogen spectra are obtained by subtracting the carbon from the CH_2 cross section and dividing by two. Figs. 4, 5, and 6 give the resultant spectra at the three angles.

As will be seen in the tables, the CH_2 peaks were examined in detail, but only one point in this energy region was measured for carbon. This is justified since the CH_2 spectrum is so intensely peaked that the exact details of the slowly changing carbon spectrum need not be known in order to get a good subtraction. At zero degrees, where the peak is analyzed in detail, there is good evidence[16] that the carbon spectrum is fairly flat from 60 to 75 Mev.

The analysis of the zero degree spectrum shows that the peak, from 65.5 to 76° Mev, is a result of deuteron formation. (See Section XI). At the other angles it is assumed that the peaks are also the result of deuteron formation. The pion energy at which the peak occurs is a function of the laboratory angle. (See Appendix I for a discussion of the dynamics of the reaction). At both 58 and 35 degrees the peaks do not fall at the calculated energy. This fact is not surprising, as the energy is a sensitive function of both the pion mass and the beam energy. The change in maximum pion energy, per Mev change in initial proton energy, varies from 0.9 Mev at zero degrees to 0.6 Mev at 58 degrees. The variation in maximum energy for a change in the pion mass of one electron mass is the same as for one Mev change in the proton energy. As the pion mass is uncertain by two electron masses, and the external proton beam is known to vary in energy by as much as 3 Mev, the energy of the peaks cannot be predicted exactly unless special precautions are taken as was done at zero degrees.

In order to obtain the cross section per unit solid angle for the formation of pions in the deuteron reaction each experimental spectrum is integrated over the energy interval of the peak. The absolute cross section is assigned a twenty percent error at zero and 35 degrees and 25 percent at the 58 degree point. Table IV shows the cross sections obtained at the different angles in the laboratory and the values after transforming to the center of mass system.

Fig. 7 shows the cross sections per unit solid angle, $d\sigma/d\Omega$, for $P + P \rightarrow \pi^+ + D$, plotted as a function of the angle of the pion in the center of mass system. It is obvious that the cross section varies with angle. The simplest assumption as to the form of the angular distribution is,

$$\frac{d\sigma}{d\Omega} = B\,(A + \cos^2\theta)\ \mathrm{cm}^2\ \mathrm{sterad.}^{-1}$$

Since the initial particles in the reaction are identical, the distribution must be symmetrical about 90 degrees; therefore, no term in odd powers of the cosine can appear. The constants A and B have been determined by the method of least squares from the data given in Table IV, giving the following result:

$$\frac{d\sigma}{d\Omega} = 3.3 \pm 1.2\ \left[.11 \pm .06 + \cos^2\theta\right] \times 10^{-29}\mathrm{cm}^2\ \mathrm{sterad.}^{-1} \qquad (10)$$

The total cross section for $P + P \rightarrow \pi^+ + D$, obtained by integrating eq. (10), is:

$$\sigma = 1.8 \pm 0.6 \times 10^{-28}\ \mathrm{cm}^2.$$

The errors given are based on the external consistency between the experimental values and the values calculated from (10). Fig. 8 shows the calculated curve and the experimental points as a function of angle in the laboratory system; for comparison a curve for a spherically symmetric distribution in the center of mass is also shown.

An independent measurement at 18 degrees in the laboratory using a liquid hydrogen target has been made by Peterson, Iloff and Sherman[17]. Their value is also shown in Fig. 8 and is in good agreement with the calculated curve.

The pion energy is also a strong function of the laboratory angle, varying by 0.8 Mev per degree at 58°. The largest possible error in the angle measurement is that at 58 degrees, where it may be as large as three degrees. However, a change in the angle of three degrees changes the constant factor in the angular distribution by only three percent, which is small compared to the uncertainties from other sources of error.

The total cross section at zero degrees, including the contribution from the continuum, is $1.9 \pm 0.4 \cdot 10^{-28}\ \mathrm{cm}^2 \cdot \mathrm{sterad.}^{-1}$.

The maximum energy of pions produced in P-P collisions depends on the proton beam energy, the direction of emission of the pions, and on the masses of proton, pion, and product nucleons. (See Appendix I). In Section XI it is shown that the peak in the spectrum is due to deuteron formation and occurs at the maximum pion energy. Thus, knowing proton and dueteron masses, it requires only a measurement of the energy of the pions in the peak, for a given proton beam energy and angle of production of the meson, in order to measure the pion mass.

The data at zero degrees was used to determine the pion mass. At zero degrees the dependence of the maximum pion energy is quite insensitive to a small variation in production angle. (See Fig. 10). The proton beam energy was measured during the zerodegree experiment by Dr. Robert Mather using the Cerenkov radiation of the beam. The energy of the pions in the peak was inferred from their range, taking into account the apparent pion energy spread introduced by the finite resolution of the apparatus. Further details can be found in reference 12.

The positive pion mass determined by this method is 275.1 ± 2.5 electron masses.

XI. DISCUSSION OF THE EXPERIMENTAL RESULTS AT ZERO DEGREES

It has already been pointed out that two reactions are possible in this experiment: (1) $P + P \rightarrow \pi^+ + D$ and (2) $P + P \rightarrow \pi^+ + N + P$.

If only reaction (2) occurs, the pion energy spectrum at any angle will consist of a continuum from zero up to some maximum energy determined by the proton beam energy and the masses of proton, neutron and pion.

The possibility that the proton and neutron come off as a deuteron was suggested in 1948 by Morand, Cuer, and Maucharafyeh[18], and in 1949 by Barkas[19]. If a deuteron is formed, the pion spectrum at any angle consists only of a line spectrum at an energy which is, because of the binding energy of the dueteron, a few Mev higher than the maximum energy pion produced by reaction (2).

Consider first the pions produced at zero degrees. The energy interval between the upper limit of the continuous spectrum (2) and the line spectrum (1) is then 4 Mev in the laboratory system. If the pion mass were known with great accuracy and if the resolution of the apparatus were sufficiently high, one could tell from the observed maximum pion energy whether or not deuteron formation ever occurred. This approach is very difficult. If, however, the shape of the experimental spectrum at zero degrees is compared with some theoretical curves given by Watson and Brueckner[20], information about the extent to which both reaction occur can be obtained.

It was pointed out by Brueckner, Chew and Hart that the production of pions in nucleon-nucleon collisions is strongly dependent on the wave-state of the product nucleons. This idea was developed by Brueckner and

Watson in their phenomenological description of the process. They give pion energy spectra at various angles for the different possibilities of wave-states for pion and product nucleons.

The outstanding feature in the experimental spectrum of pions produced at zero degrees by protons on protons is the intense peak near maximum meson energy. The shape of the spectrum near the peak is primarily determined, in the theory, by the wave functions of the nucleons in the final state. It might be expected that for those pions produced with energies near the maximum, the product-nucleons would be in an S-state, since their relative velocity is small. And indeed, the experimental results do not fit any of the theoretical spectra of Brueckner and Watson based on the assumption that the final nucleons are in a P-state.

According to the theory, a strong peak will occur if the nucleons come off in either a triplet S-state or in a singlet S-state. If the product nucleons come off in a ^{3}S-state, there is a large probability that pion production will be accompanied by deuteron formation. The resulting line spectrum will be intense compared to the continuum, thus giving rise to the peak. If, however, the nucleons are left in the ^{1}S-state, a strong peak will still arise because of the resonance resulting from the low energy virtual state of the deuteron.

It should be pointed out that deuterons have been detected in coincidence with pions of ppproximately maximum energy by Crawford, Crowe and Stevenson.[21]

It can be concluded from the results at zero degrees that the peak in the spectrum is due solely to deuteron formation. This follows from a comparison of the experimental points with the curves derived by folding the resolution of the apparatus (see Appendix II) into the theoretical spectra.

Curve II, Fig. 9, shows the result of folding the resolution into that theoretical spectrum in which the nucleons are left in the ^{1}S-state and the pions are produced in a P-state with a $\cos^2\theta$ distribution in the center of mass system. As mentioned above, the shape of the spectrum at the peak is primarily determined just by the final state of the nucleons. This choice for the pion wave-state, however, gives the best of the theoretical spectra based on the ^{1}S-state to the experimental points in the peak.

Curve I, of Fig. 9, shows the result of folding the resolution into that spectrum in which the nucleons are left in the ^3S-state, and the pions are again produced in a P-state with a $\cos^2\theta$ distribution. Since the main feature of this spectrum is a line displaced upward by 4 Mev from the continuum, this curve is essentially a plot of the estimated resolution. The resolving power is sufficiently high, as shown in Appendix II, that the apparatus does not appreciably mix the continuum and the line spectrum. The selection of the particular angular momentum and angular distribution of the pions is even less critical here than for the ^1S case, since the intense deuteron peak is the essential feature of all the ^3S spectra.

Fig. 9 also shows the experimental points at zero degrees. Both theoretical curves are normalized so that in each the area from 65.5 to 76.0 Mev agrees with the area under the experimental points in the same energy interval. The close fit of curve I with the experimental results is strong evidence that the peak corresponds to deuteron formation. It is clear that the experimental points, on the other hand, are not in agreement with either the half-width or the asymmetric character of Curve II for the ^1S case.

The experimental results thus establish that the peak is largely due to deuteron formation. There is still the possibility to be examined that the peak contains an appreciable contribution from ^1S final nucleon states. However, the ^1S peak contribution will occur 4 Mev below the contribution from the ^3S deuteron line. Since, as mentioned above, the resolving power of the apparatus is high enough to distinguish details in the spectrum that are 4 Mev apart, any appreciable ^1S contribution would have occurred in the experimental results as a separate peak 4 Mev below that of the deuterons. Therefore, it can be concluded that the intense peak is due entirely to deuteron formation.

Since the peak accounts for approximately 70 percent of the total cross section at zero degrees, it is clear that roughly 70 percent of the mesons produced at zero degrees are accompanied by nucleons in the ^3S-state.

The observed angular distribution implies that the mesons associated with the $P + P \rightarrow \pi^+ + D$ reaction are largely in a P-state with, possibly, a small amount of S-state.

Recent experiments suggest that the pion is pseudoscalar.[22] Using the Pauli exclusion principle and conservation of parity and angular momentum, it then follows that if the pion is in an S-state, the nucleons are

in a ^1S_o-state, while if the pion is in a P-state, the nucleons are in a $^3S_1$-state. Thus, the conclusions from the 0° data are consistent with the results from the angular distribution.

That the pions come off largely in a P-state is also consistent with another experimental result. Brueckner and Watson point out that if in the production of neutral pions in proton-proton collisions the pions go off primarily in a P-state, then by conservation of parity and angular momentum one obtains, using the Pauli exclusion principle, a strict selection rule forbidding the reaction if the pion is pseudoscalar. This is in agreement with the experiments of Hales, Hildebrand, Knable and Mouer,[23] who find an extremely low yield of neutral pions when hydrogen is bombarded by 340 Mev protons.

XII. SPIN OF THE POSITIVE PION

The principal reaction studied in this experiment is $P + P \rightarrow \pi^+ + D$. In the center of mass system the pion energy is 21.4 Mev for an initial proton energy in the laboratory of 341 Mev. If the cross section for the absorption of a 21.4 Mev pion by a deuteron to give two protons is also known, the spin of the pion can be calculated by the principle of detailed balance.[24] Assuming that the initial protons in one case, and the initial pions in the reverse reaction are unpolarized, we can write,

$$\left(\frac{d\sigma}{d\Omega}\right)_P = \frac{(2S_P+1)^2\, p^2}{(2S_D+1)\,(2S_\pi+1)\quad q^2} \left(\frac{d\sigma}{d\Omega}\right)_{\pi+} \qquad (11)$$

where $(d\sigma/d\Omega)_P$ is the cross section for producing a proton in a unit solid angle from the absorption of a pion, S_P, S_D, and S_π are the spins of the proton, deuteron, and pion respectively, and p and q are the proton momentum and pion momentum respectively in the c.m. system.

The pion absorption cross section has been measured by Durbin, Loar, and Steinberger[25] at Columbia University and by Clark, Roberts and Wilson[26] at the University of Rochester. In the Columbia experiment the cross section has been measured as a function of proton angle at pion energies ranging from 25 to 53 Mev. In the Rochester experiment the angular distribution could not be obtained, but the total cross section was calculated for various values of the constant, A is the assumed angular distribution, $B(A + \cos^2\theta)$. Their result is an average over pion energies from 0 to 30 Mev.

The decay scheme of the positive pion and the mode of absorption of the negative pion are good evidence that the pion spin must be integral.[22] Comparison of the experiment at Berkeley by means of the principle of detailed balance with those at Columbia and Rochester makes it possible to choose between the values of zero or one for the spin.

In Table V the cross sections are listed for the process $\pi^+ + D \rightarrow P + P$. The Berkeley values were calculated using eq. (11), (a) with the spin of the pion equal to zero, and (b) with the spin equal to one. The total cross section quoted from Rochester is based on the assumed angular distribution, $0.2 + \cos^2\theta$. The total cross sections from Berkeley and Columbia are in good agreement for pion spin zero, although the angular distributions differ somewhat. The Rochester cross section, although more than one probable error away from the Berkeley result for spin zero, is in a direction opposite to that expected for spin one. With pion spin equal to unity, the Berkeley measurement yields a $\pi^+ + D \rightarrow P + P$ cross section which is about seven probable errors lower than the direct Columbia measurement, and four probable errors lower than the Rochester measurement.

The excitation function of this reaction is a strong function of energy. The difference in the experimental energies and their uncertainty, thus introduce some ambiguity in the above comparisons. The excitation function at zero degrees has been measured up to a proton energy of 341 Mev by Schulz[27] and in the inverse experiment from a pion energy of 25 to 53 Mev by Durbin, et al. Using their data it would appear that transforming the Columbia result to the lower pion energy would at most lower it by 30 percent. A change of this magnitude would leave the conclusions as to the spin unchanged.

Thus, on the basis of the experiments done to date one can conclude that the pion spin is very probably zero. The experiments of Panofsky, Aamodt and Hadley[22] on the pion absorption in deuterium show that if the negative pion has spin zero, it cannot be a scalar particle. Assuming that the positive and negative pions are particles of like character, it can be concluded that the charged pions are pseudoscalar.

ACKNOWLEDGMENTS

It is a great pleasure for us to thank Professor Ernest O. Lawrence, for his interest and encouragement.

Many helpful and stimulating discussions were held with Dr. Kenneth M. Watson and Dr. Miriam Cartwright. We would also like to thank Mr. James Vale and the cyclotron crew for making the bombardments, and Mr. Dan Hamlin and Mr. Otto Heinz for their help in various portions of the experiment which contributed substantially to its successful completion.

APPENDIX I. DYNAMICS

The relativistic calculations for the dynamics of reaction (1) and (2) are easily made. Let T be the kinetic energy of the protons in the laboratory. Then the velocity of the center of mass in units of c, β_{cm}, is given by the formula

$$\beta_{cm} = T^{1/2} (2R_p + T)^{-1/2} \tag{I-1}$$

Let $\gamma_{cm} = (1 - \beta^2_{cm})^{-1/2}$; then the total energy available in the center of mass system, U, is given by

$$U = 2R_p\gamma_{cm} = \left[2R_p (2R_p + T)\right]^{1/2} \tag{I-2}$$

In the center of mass system, the pions come off in reaction (1) with total energy (rest + kinetic) given by:

$$E_\pi' = \frac{U}{2} - \frac{R_D^2 - R_\pi^2}{2U} \tag{I-3}$$

where R_D and R_π are the rest energies of the deuteron and pion respectively. The maximum pion energy in reaction (2) is obtained by substituting the rest energy of the neutron plus proton for the rest energy of the deuteron in the last formula. If the pion comes off at an angle θ' to the beam in the c.m. system, then in the laboratory the angle with respect to the beam, θ, is given by the well known formula;

$$\tan\theta = \frac{\beta_\pi' \sin\theta'}{\gamma_{cm} (\beta_\pi' \cos\theta' + \beta_{cm})} \tag{I-4}$$

where β_π' is the velocity of the pion, in units of c, in the c.m. system. The total energy of the pion in the laboratory, E_π, is given as a function of θ by the formula:

$$E_\pi = (\gamma_{cm} b)^{-1} (E_\pi' + \beta_{cm} \cos\theta \sqrt{E_\pi'^2 - \gamma^2_{cm} b R_\pi^2}) \tag{I-5}$$

where $b = 1 - \beta^2_{cm} \cos^2\theta$.

Fig. 10 is a plot of eq. (I-5) for the case in which a deuteron is formed and also for the case in which the neutron and proton come off unbound and the pion is emitted with maximum energy.

The relation between the elements of solid angle in the laboratory, $d\Omega$, and the corresponding element of solid angle in the center of mass, $d\Omega'$, is given by the formula

$$\frac{d\Omega}{d\Omega'} = \frac{p_\pi'}{p_\pi^3 c^2} \left(E_\pi E_\pi' - \gamma_{cm} R_\pi^2 \right). \qquad \text{(I-6)}$$

p_π and p_π' are the momenta of the pion in the laboratory and in the c. m. system, respectively.

At zero degrees and for 340 Mev protons and a pion mass of 275.1 electron masses, $dE_\pi/dE_p = 0.9$ and $(dE_\pi/dm_\pi) = 0.8$ Mev per electron mass.

APPENDIX II. RESOLUTION

The experimental energy spectrum of the pions was determined from the density of pion endings found at each depth in the absorber. The density of pions as a function of range was then converted to the density of pions as a function of energy by means of the range-energy curves for pions. This method of detection introduces a finite resolving power into the apparatus. Pions of a particular energy will not have a unique depth of penetration into the absorber because of range straggling and multiple small angle scattering. The first effect is due to the statistical fluctuations in the number of collisions the pion undergoes, and gives an approximately gaussian distribution in range. The multiple Coulomb scattering gives rise to a distribution in depth of penetration for pions of the same range because the projected range depends on the angles through which each pion has been scattered in the course of its travel through the absorber. Since the energy of a pion was deduced from the position of its ending in the absorber, the above variation in depth of penetration for a monoenergetic beam of pions will manifest itself as an apparent spread in the energies of the pions coming to the absorber.

Further energy smearing arises because the detector accepts mesons from a small range of angles about zero degrees, and the pion cut-off energy or peak energy, in which we are interested, varies with the angle of production. The geometry of the zero degree experiment allowed a variation in angle, for the maximum energy pions, from -3° to -3°. As is shown in Fig. 10 this introduces a spread in energy of less than 0.2 Mev. Therefore, this effect can be neglected in determining the resolving power.

The use of a thick target would also be expected to decrease the resolving power. However, for the pions of maximum energy, this turns out to give only a spread of 0.1 Mev for the thickness of CH_2 used in the experiment. This comes about in the following way: While the pions at the front of the target lose a small amount of their energy in traversing the target, the protons also lose energy in passing through the target, and produce pions of correspondingly lower energy at the back of the target. Thus, the energy loss in the target by the pions tends to be compensated by the energy loss of the protons.

The main causes of the finite resolving power introduced by the detection method are, therefore, the multiple small angle scattering and the range straggling mentioned above. An additional energy spread is introduced into the experiment by the proton beam, which is itself not monoenergetic. The energy distribution of maximum energy pions arising from each of these three effects has been calculated below. The three distributions are then folded together. The resulting curve, shown in Fig. 11, gives the distribution in energy that maximum energy pions produced in a proton-proton collisions will appear to have, when produced at 0° and detected with the experimental equipment used.

The resolution has been assumed to be constant over the high energy part of the spectrum in obraining the curves in Figs. 4 and 9.

The depth of penetration for a monoenergetic beam of pions entering an absorber normally will have a distribution, due to scattering, which is calculated approximately below.

A collimated monoenergetic beam of pionswill, after passing through an absorber of thickness dx, possess a gaussian distribution of angles due to multiple small angle scattering. The mean square angular spread is[28]

$$\overline{\phi^2} = \frac{16\pi N Z^2 e^4 dx}{v^2 p^2} \ln (181\, Z^{-1/3}) = \frac{C\, dx}{v^2 p^2} \qquad \text{(II-1)}$$

where $C = 16\pi N Z^2 e^4 \ln (181\, Z^{-1/3})$, and where N is the number of atoms per cm^3 of the absorber, Ze is the atomic charge of the absorber material, e is the electronic charge, and v and p are the velocity and momentum of the pion respectively.

Using eq. (8) we find that a pion following the rms angle of deflection in each thickness dx of the absorber, will have, at a depth x in the absorber, a direction of travel given approximately by $\Theta_{rms}(x)$, where

$$\overline{\Theta^2}(x) = \frac{0.31\, C}{k^2 (2n - 1)} \left[(R_o - x)^{1-2n} - R_o^{\,1-2n} \right] \qquad \text{(II-2)}$$

This formula is not applicable at $x = R_o$ where the small angle scattering formula (II-1) does not hold. However, for an aluminum abosrber, $\sqrt{\overline{\Theta^2}(x)}$ is about 22° at $x = 0.99\, R_o$. The assumption of small angle scattering is therefore valid in the interval $x = 0$ to $x = 0.99\, R_o$. Since almost all of the variation in depth of penetration of the pions takes place in this interval, eq. (II-2) should be accurate, for our purposes, to within about 20 percent.

Now, in order to obtain the distribution in depth from the expression for Θ^2_{rms}, we introduce the assumption that a pion at a depth x' whose trajectory makes an angle $\Theta(x') = k\,\Theta_{rms}(x')$ with the forward direction, will at all x, maintain a direction of travel given by $\Theta(x) = k\,\Theta_{rms}(x)$. Thus, on this assumption, a pion traveling at an angle equal to twice the r.m.s. angle, always travels at twice the r.m.s. angle. This assumption is not unreasonable for obtaining a rough idea of the distribution. An exact treatment of the problem seems difficult. On the other hand, the above assumption leads to a distribution in depth of penetration, which, although crude, seems more realistic than assuming, for example, a constant "average" decrease in depth of penetration for each pion.

Since the distribution in $\Theta(x)$ is gaussian, the distribution in k is also gaussian, and the fraction of the total number of pions with k in dk is

$$N(k)\,dk = \frac{2}{\sqrt{2\pi}}\, e^{-k^2/2}\, dk.$$

Knowing, at every depth x, the angle with which each pion travels relative to the original direction, we are able to compute each path.

The path length traversed by a pion is $\int (dx/\cos\Theta(x))$, and the shortening in the projected path distance is therefore, given approximately by $\omega = \int_0^R (dx\,\Theta^2(x)/2)$.

The average shortening that the projected paths undergo is given by the shortening for the pion which maintains the r.m.s. angle. Using eq. (II-2) this average shortening, ω^*, turns out to be $.08C/(1-n)\cdot R_o^2/T_o^2$, where T_o is the initial kinetic energy of the pion.

The pion maintaining the direction of travel $k\,\Theta_{rms}(x)$ has then a decrease of penetration given by $\omega = k^2\omega^*$. The distribution in ω is found from the distribution in k:

$$N(\omega)\,d\omega = \frac{e^{-\omega/2\omega^*}}{\sqrt{2\pi\,\omega\,\omega^*}}\, d\omega \qquad \text{(II-3)}$$

With the absorbers used, the total shortening in depth of penetration was, for the "rms" pion, 0.14 cm of aluminum. Since the energy is inferred from the depth of penetration, a pion traveling along the path with the rms angle will appear to have an energy decreased from the true energy by $\omega^*\,(-dE/dx)\,\mathrm{Al},\,T_o$. This yields $\Delta E^* = 0.88$ Mev. The distribution in ω, (eq. II-3) corresponds to a distribution in E given by:

$$N(E)dE = \frac{e^{-(E_o-E)/2\ (0.88)}}{\sqrt{2\pi\ (E_o-E)\ \ 0.88}}\qquad dE \tag{II-4}$$

where E_o is the true pion energy and the energies are in Mev.

Next, the effect on the energy resolution of range straggling due to statistical fluctuations in the number of collisions that the meson undergoes. Livingston and Bethe[29] give an expression for the mean square width in the gaussian distribution of distance traveled by monoenergetic particles which lose a given amount of energy by ionization. For pions of high velocity which decrease in energy from E_1 to E_2 this expression yields:

$$\overline{\Delta R^2} = \int_{E_2}^{E_2} \frac{4\pi e^4 NZ}{\left(\frac{-dE}{dx}\right)^3}, \qquad dx \tag{II-5}$$

where e is the electronic charge, N is the number of atoms per cubic centimeter of the absorber, Z is the number of electrons per atom that are effective in the ionization process, and $(-dE/dx)$ is the rate of energy loss of the pion at the energy E. The integration can be carried out by means of eq. (8). For the experimental absorbers used, the total accumulated straggling in range was calculated as $\Delta R_{rms} = 0.15$ cm of Al. If there were no straggling, this gaussian distribution in range would correspond to a gaussian distribution in the energy with which the pions enter the absorber. The mean square in this energy distribution is given by:

$$\overline{\Delta E^2} = \left(\frac{dE}{dx}\right)^2_{E_o} \qquad \overline{\Delta R^2} = 0.92\ \text{Mev}^2.$$

The electrically deflected 341 Mev proton beam has an energy spread estimated to be about 1.6 Mev. Without a detailed analysis of the origin of this spread, we have assumed that the distribution in energies is gaussian with an r.m.s. spread of 1.2 Mev. This value gives the best fit to the experimental points. If, however any value in the vicinity of 1.5 Mev were used for the r.m.s. spread, the conclusions reached would remain unchanged.

Protons with a gaussian energy distribution will produce pions whose maximum energy will also have a gaussian distribution. Since a change in proton energy of 1 Mev produces a change of 0.9 Mev in the maximum pion energy, the pion energy gaussian will have an r.m.s. width of 0.9 x 1.2 or 1.08 Mev.

The range straggling and proton beam energy distributions, when folded together, give a gaussian of r.m.s. width 1.44 Mev. The final resolution curve is found from folding the distribution produced by multiple Coulomb scattering into this gaussian, and is plotted in Fig. 11.

TABLE I

Target	Pion Energy, Mev	$d\sigma/dEd\Omega \times 10^{30}$ (Uncorrected), cm^2 Mev^{-1} $ster^{-1}$	Correction Factors			$d\sigma/dEd\Omega \times 10^{30}$ (Corrected), cm^2 Mev^{-1} $ster^{-1}$	Statistical Probable Error x 10^{30} cm^2 Mev^{-1} $ster.^{-1}$
			Decay in Flight	Thick Target	Attenuation in Absorber		
CH_2	17.5	3.0	1.13	1.11	1.02	3.8	±0.6
Carbon	17.5	1.9	1.13	1.12	1.02	2.5	±0.3
CH_2	34.0	5.3	1.09	1.11	1.05	6.7	±0.7
Carbon	34.0	3.3	1.09	1.12	1.05	4.3	±0.4
CH_2	60.9	13.3	1.08	1.01	1.14	16.5	±0.9
CH_2	63.8	11.8	1.08	1.01	1.16	14.9	±1.4
CH_2	65.7	13.8	1.08	1.01	1.16	17.5	±1.9
CH_2	67.2	22.8	1.08	1.01	1.17	29.1	±2.0
CH_2	68.8	45.4	1.08	1.01	1.18	58.5	±2.4
Carbon	70.0	9.2	1.07	1.02	1.18	11.8	±1.3
CH_2	70.7	50.5	1.07	1.01	1.18	64.4	±2.6
CH_2	72.3	18.7	1.07	1.01	1.19	24.0	±2.1
CH_2	73.7	11.2	1.07	1.01	1.20	14.5	±1.8
CH_2	75.6	10.9	1.07	1.01	1.22	14.4	±1.9

TABLE II

Target	Pion Energy, Mev	$d\sigma/dE d\Omega \times 10^{30}$ (Uncorrected), cm^2 Mev^{-1} $ster^{-1}$	Attenuation in Absorber	$d\sigma/dE d\Omega \times 10^{30}$ (Corrected), cm^2 Mev^{-1} $ster^{-1}$	Statistical Probable Error, cm^2 Mev^{-1} $ster.^{-1}$
CH_2	40.2	7.70	1.08	9.0	±0.62
	42.8	9.97	1.09	11.7	±0.83
	43.8	16.6	1.09	19.7	±1.3
	44.6	19.4	1.09	23.1	±1.6
	45.3	22.8	1.09	27.3	±1.9
	46.0	25.8	1.10	31.2	±2.0
	46.9	26.6	1.10	32.2	±2.1
	47.7	21.3	1.10	25.8	±1.6
	48.3	16.0	1.10	19.4	±1.4
	49.7	8.52	1.10	10.3	±0.94
	50.5	5.31	1.11	6.5	±0.54
C	44.0	5.49	1.08	6.46	±0.45

TABLE III

Target	Pion Energy, Mev	$d\sigma/dE d\Omega \times 10^{30}$ (Uncorrected), cm^2 Mev^{-1} $ster^{-1}$	Thick Target Correction Factor	$d\sigma/dE d\Omega \times 10^{30}$ (Corrected), cm^2 Mev^{-1} $ster^{-1}$	Probable Error $\times 10^{30}$ cm^2 Mev^{-1} $ster^{-1}$
CH_2	20.0	3.03	1.11	3.8	±0.4
	21.0	3.16	1.09	3.8	±0.4
	22.5	3.98	1.08	4.7	±0.4
	24.5	6.81	1.07	8.0	±1.0
	25.0	6.19	1.07	7.3	±0.7
	27.0	4.30	1.07	5.1	±0.7
	28.5	2.70	1.06	3.2	±0.6
C	26.0	3.21	1.08	3.8	±0.3

TABLE IV

$\theta_{lab.}$	$(d\sigma/d\Omega)_{lab.} \times 10^{28}$, cm^2 ster.$^{-1}$	$\theta_{c.m.}$	$(d\sigma/d\Omega)_{c.m.} \times 10^{29}$, cm^2 ster.$^{-1}$
8°	1.2 ±0.25	0°	3.1 ±0.7
35°	0.50±0.10	65°	1.8 ±0.4
58°	0.08±0.02	104°	0.47±0.12

TABLE V

Experiment		T_π(c.m.), Mev	$(d\sigma/d\Omega)_p \times 10^{28}$, cm^2 sterad.$^{-1}$	$\sigma_{tot.} \times 10^{27}$, cm^2
Berkeley	a	21.4	11±4(0.11±.06+$\cos^2\theta$)	3.0±1.0
	b		3.7±1.3(0.11±.06+$\cos^2\theta$)	1.0±0.3
Rochester		23 (ave.)		4.5±0.8*
Columbia		25	9(0.22+$\cos^2\theta$)	3.1±0.3

* Assuming an angular distribution of (0.2+$\cos^2\theta$), see ref. 26.

a) Transformed on the assumption that $S_\pi = 0$.

b) Transformed on the assumption that $S_\pi = 1$.

TITLES FOR THE FIGURES

Fig. 1: Schematic diagram of the experimental set-up.

Fig. 2: A) The position of nuclear emulsion in the absorber.
B) The composite absorber used to obtain the zero degree data.

Fig. 3: Diagram used to calculate the flux of pions from the density of stopped pions in the emulsion. See Section IX.

Fig. 4: Differential cross section, as a function of pion energy, for pion production from hydrogen at zero degrees. The solid curve results from folding the experimental resolution into the theoretical spectrum for the final nucleons in a ^3S-state and the pion in a P-state with a $\cos^2\theta$ angular distribution in the c.m. system. (See Section XI).

Fig. 5: The differential cross section in the region of the peak for pion production from hydrogen at 35° as a function of the energy.

Fig. 6: The differential cross section in the region of the peak for pion production from hydrogen at 58°.

Fig. 7: Angular distribution in the center of mass system of the pions in the peak. The solid curve is a least squares fit of the data.

Fig. 8: Angular distribution of the pions in the peak vs. laboratory angle. The solid curve comes from a least squares fit of the data in the c.m. system. The dashed curve is the result of transforming to the laboratory a uniform angular distribution in the c.m. system.

Fig. 9: Experimental points and theoretical curves for the differential cross section for pion production from hydrogen at 0° in the neighborhood of the peak. Curve 1: the nucleons are left in the ^3S-state and the pions are produced in a P-state with a $\cos^2\theta$ distribution in the c.m. system. Curve 2: the nucleons are left in the ^1S-state and the pions are produced in a P-state with a $\cos^2\theta$ distribution intthe c.m. system.

Fig. 10: Kinetic energy of the pion vs. angle in the laboratory. The solid curve is for the case in which a deuteron comes off. The dashed curve is the maximum energy of the pion when a neutron and proton come off.

Fig. 11: Resolution of the apparatus for the zero degree experiment.

TITLES FOR THE TABLES

Table I: Results at 0°.

Table II; Results at 35°. The correction factor for decay in flight is 1.07. The correction for the thickness of the target is negligible here.

Table III: Results at 58°. The correction factors for decay in flight and for attenuation in the absorber are 1.06 and 1.04 respectively.

Table IV: Summary of the measured cross sections for the reaction $P + P \rightarrow \pi^{+} + D$.

Table V: Comparison of the cross sections for pion absorption by deuterium as obtained by Clark, Roberts and Wilson at Rochester and Durbin, Loar, and Steinberger at Columbia, with the present results, which have been transformed to give the absorption cross section by the principle of detailed balance.

REFERENCES

1. C. Richman, and H. A. Wilcox; Phys. Rev. 78, 496 (1950).
2. M. Weissbluth, Ph.D. Thesis, Univ. of Calif., (1950).
3. W. F. Cartwright, C. Richman, M. N. Whitehead and H. A. Wilcox, Phys. Rev. 78, 823 (1950).
4. K. A. Brueckner, Phys. Rev. 82, 598 (1951). (In particular see appendix by Brueckner, Chew and Hart.
5. M. H. Johnson, Private communication to R. E. Marshak
6. R. E. Marshak, Rochester High Energy Conference, Dec. (1951) (unpublished) W. B. Cheston, Phys. Rev. 83, 1118 (1951).
7. See e.g. W. M. Powell, L. R. Henrich, Q. A. Kerns, D. C. Sewell, and R. L. Thornton R.S.I. 19, 506 (1948) for a description of the deflecting mechanism and J. B. Cladis, W. N. Hess, and B. J. Moyer, Phys. Rev. 87, 425 (1952) for a description of the collimating system.
8. C. Richman, M. Weissbluth, and H. A. Wilcox, Phys. Rev. 85, 161 (1952).
9. W. A. Aron, B. G. Hoffman, and F. C. Williams, AECU-663, unpublished.
10. R. Mather and E. Segre, Phys. Rev. 84, 191 (1951).
11. W. H. Barkas, unpublished.
12. For details, see UCRL-1278, Office of Technical Services, Dept. of Commerce, Wash., D. C.
13. O. Chamberlain, R. F. Mosley, J. Steinberger, and C. Wiegand, Phys. Rev. 79, 394 (1950).
14. See for example, H. Bradner, F. M. Smith, W. H. Barkas, and A. S. Bishop, Phys. Rev. 77, 462 (1950).
15. D. Stork, Meeting of the American Physical Society, Dec. 1952.
16. W. Dudziak, to be published.
17. V. Z. Peterson, E. Hoff and D. Sherman, Phys. Rev. 81, 647 (1951).
18. J. Morand, P. Cuer, and H. Maucharafyeh, Compt. Rend. 226, 1974 (1948).
19. W. Barkas, Phys. Rev. 75, 1109 (1949).
20. K. M. Watson and K. A. Brueckner, Phys. Rev. 83, 1 (1951). See also K. M. Watson, Phys. Rev. 88, 1163 (1952).
21. F. S. Crawford, K. M. Crowe, and M. L. Stevenson, Phys. Rev. 82, 97 (1951).
22. W. K. H. Panofsky, R. L. Aamodt, and J. Hadley, Phys. Rev. 81, 565 (1951).
23. R. W. Hales, R. H. Hildebrand, N. Knable and B. J. Moyer, Phys. Rev. 85, 373 (1952).

24. See e.g. H. A. Bethe, Elementary Nuclear Physics, p. 61, John Wiley and Sons, Inc., New York, (1947).

25. R. Durbin, H. Loar, and J. Steinberger, Phys. Rev. 83, 646 (1951) and Phys. Rev. 84, 581 (1951).

26. D. L. Clark, A. Roberts and R Wilson, Phys. Rev. 83, 649 (1951) and Phys. Rev. 85, 523 (1952).

27. A. G. Schulz Jr. UCRL-1756.

28. Rossi and Greisen, Rev. Mod. Phys. 13, 263 (1941).

29. M. S. Livingston and H. A. Bethe, Rev. of Mod. Phys. 9, 245, (1937).

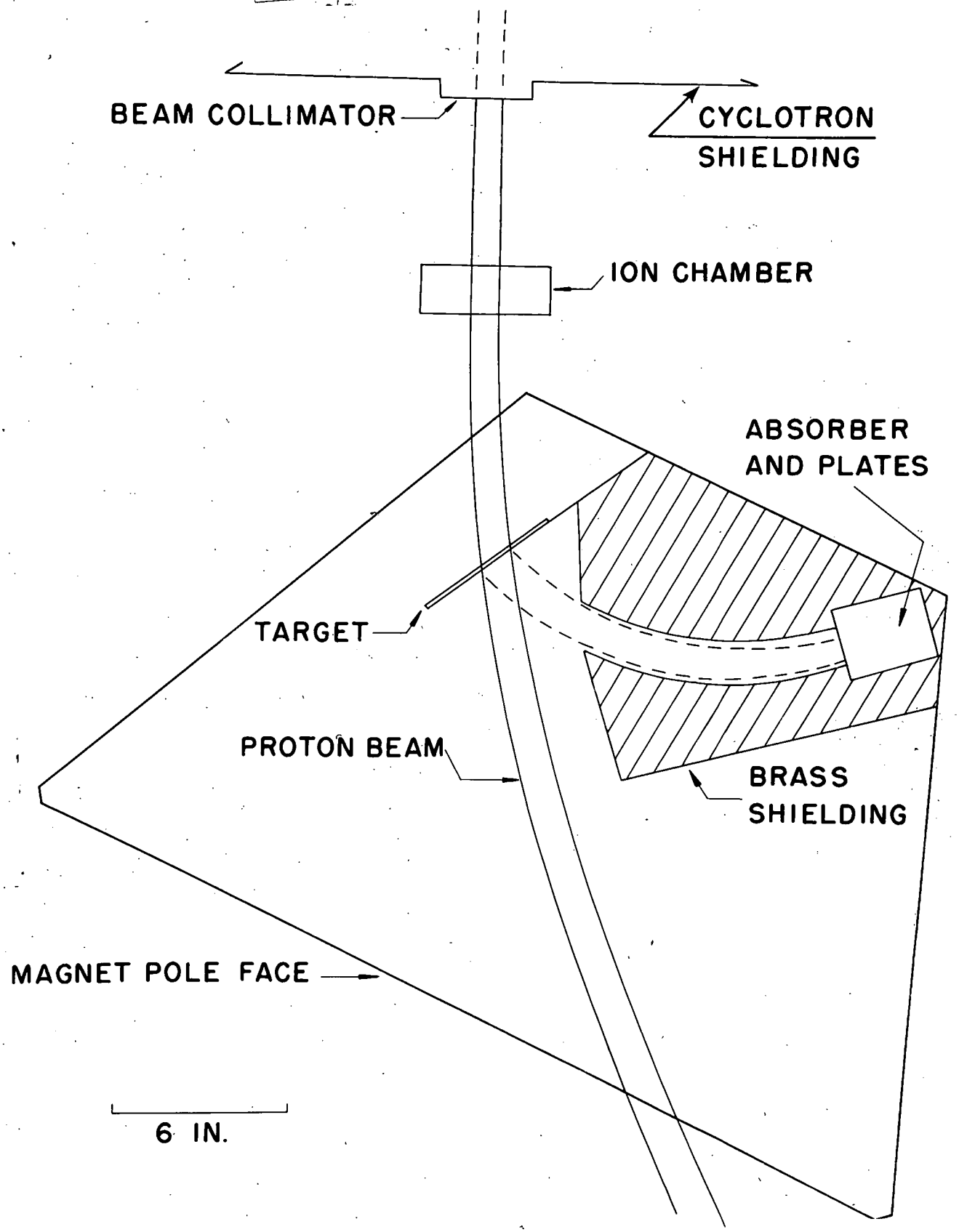
BEAM COLLIMATOR
CYCLOTRON
SHIELDING
ION CHAMBER
ABSORBER
AND PLATES
TARGET
PROTON BEAM
BRASS
SHIELDING
MAGNET POLE FACE
6 IN.

FIG. 1

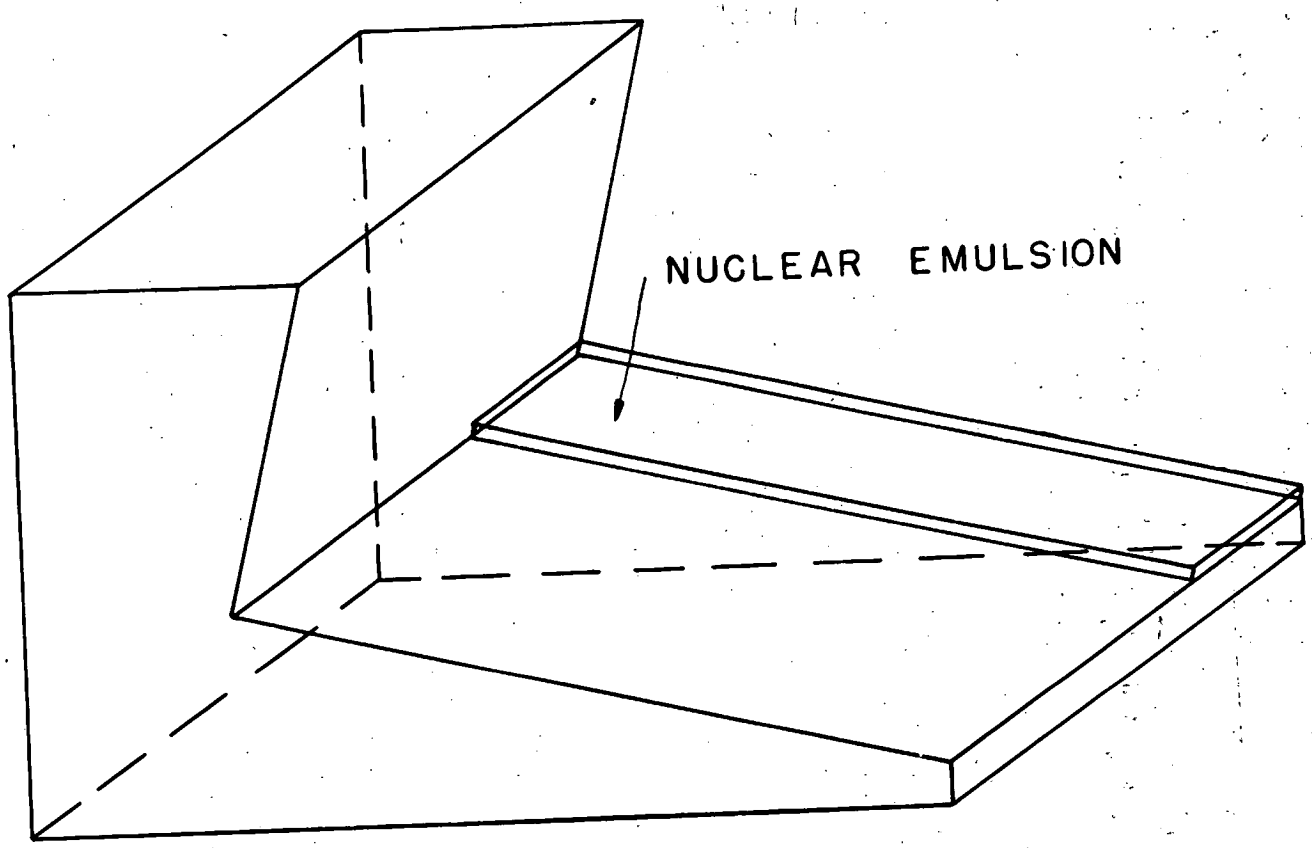

A)

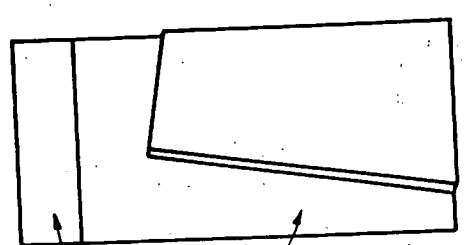

B) Cu Al

FIG. 2

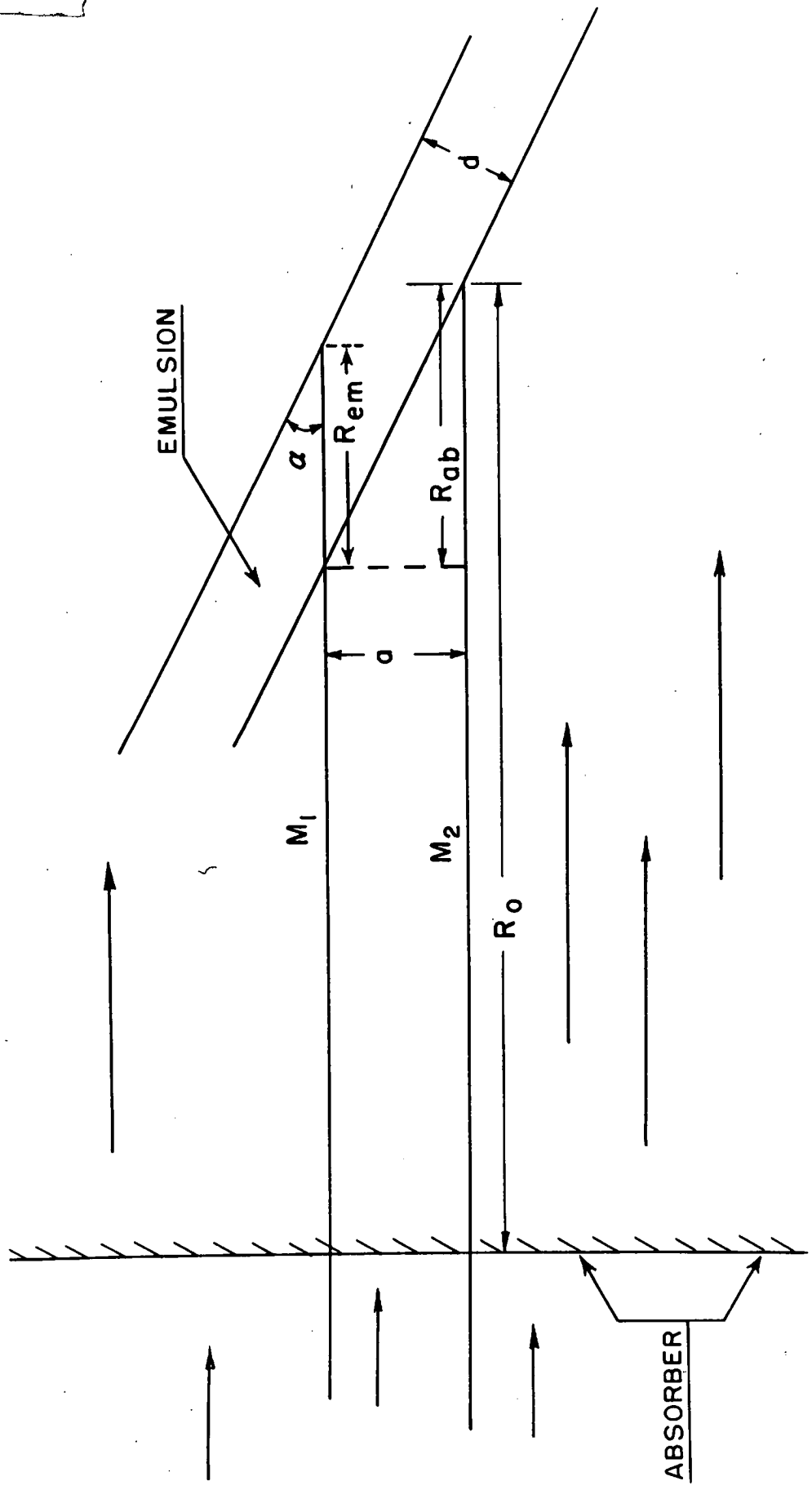

FIG. 3

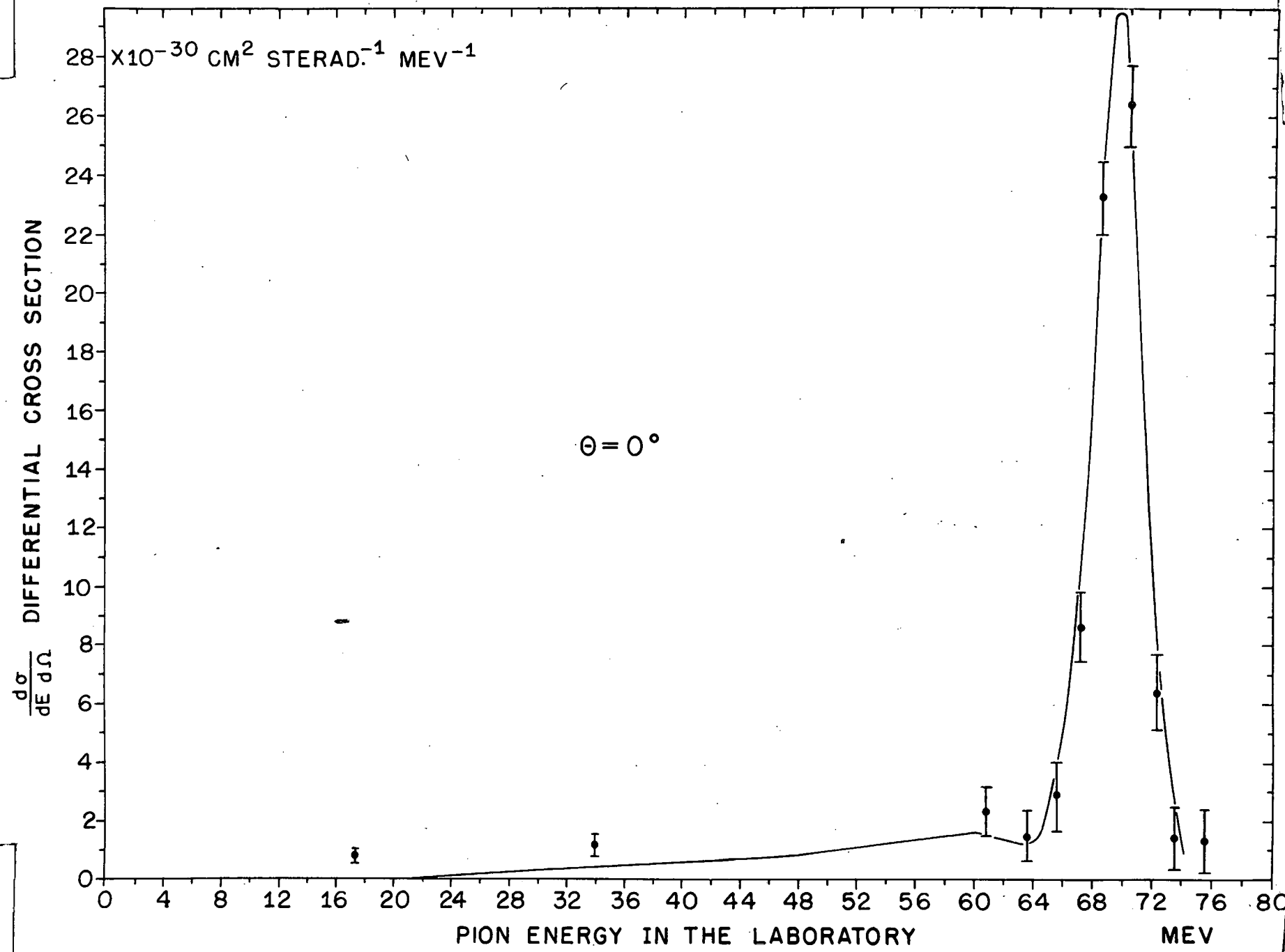
X10^{-30} CM^2 STERAD.$^{-1}$ MEV^{-1}
$\frac{d\sigma}{dE\,d\Omega}$ DIFFERENTIAL CROSS SECTION
Θ = 0°
0
2
4
6
8
10
12
14
16
18
20
22
24
26
28
0 4 8 12 16 20 24 28 32 36 40 44 48 52 56 60 64 68 72 76 80
PION ENERGY IN THE LABORATORY
MEV

Fig. 4

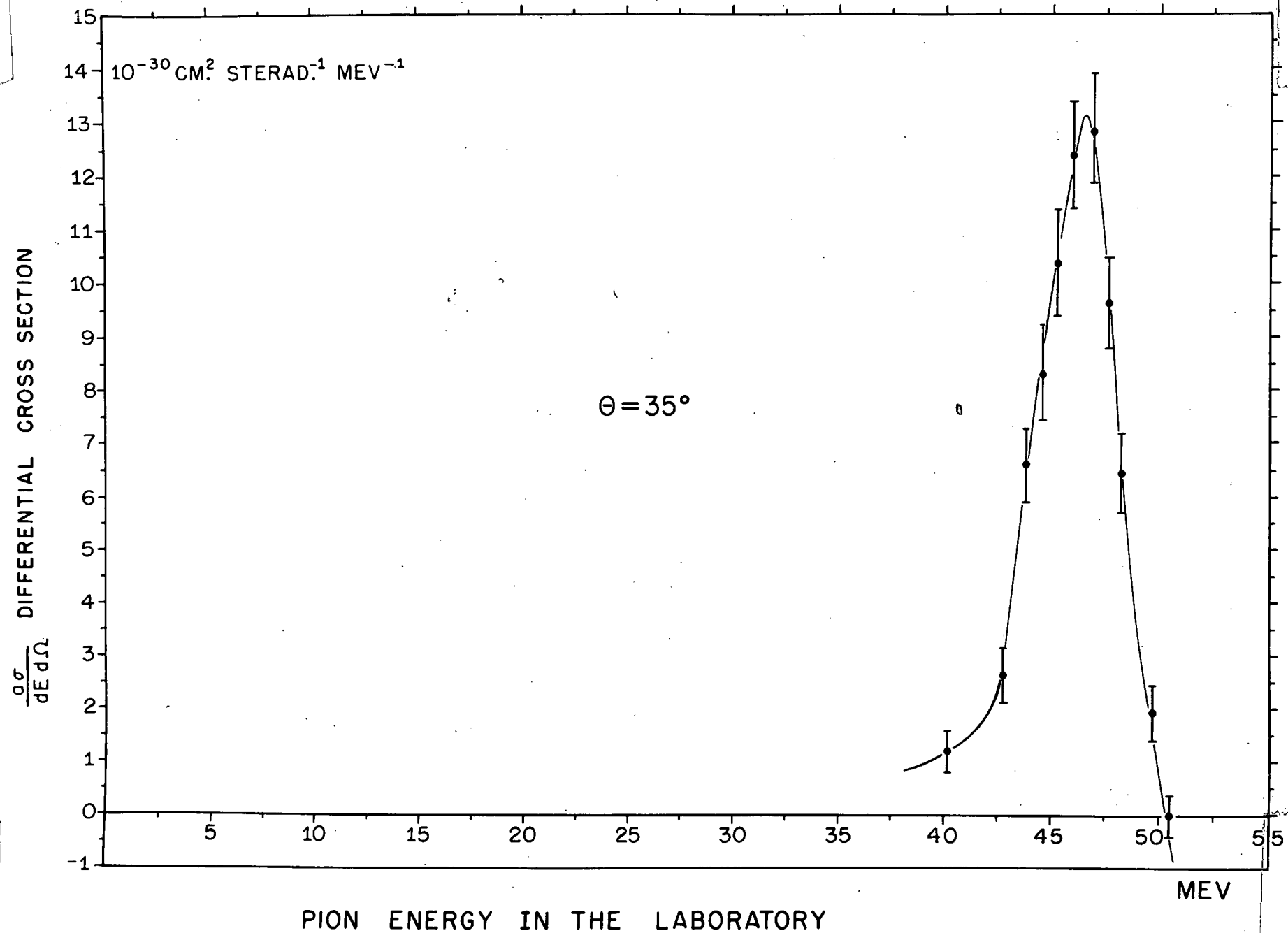
10^{-30} CM.^{2} STERAD.$^{-1}$ MEV^{-1}
$\Theta = 35°$
$\frac{d\sigma}{dE\,d\Omega}$ DIFFERENTIAL CROSS SECTION
15
14
13
12
11
10
9
8
7
6
5
4
3
2
1
0
-1
5
10
15
20
25
30
35
40
45
50
55
MEV
PION ENERGY IN THE LABORATORY

Fig. 5

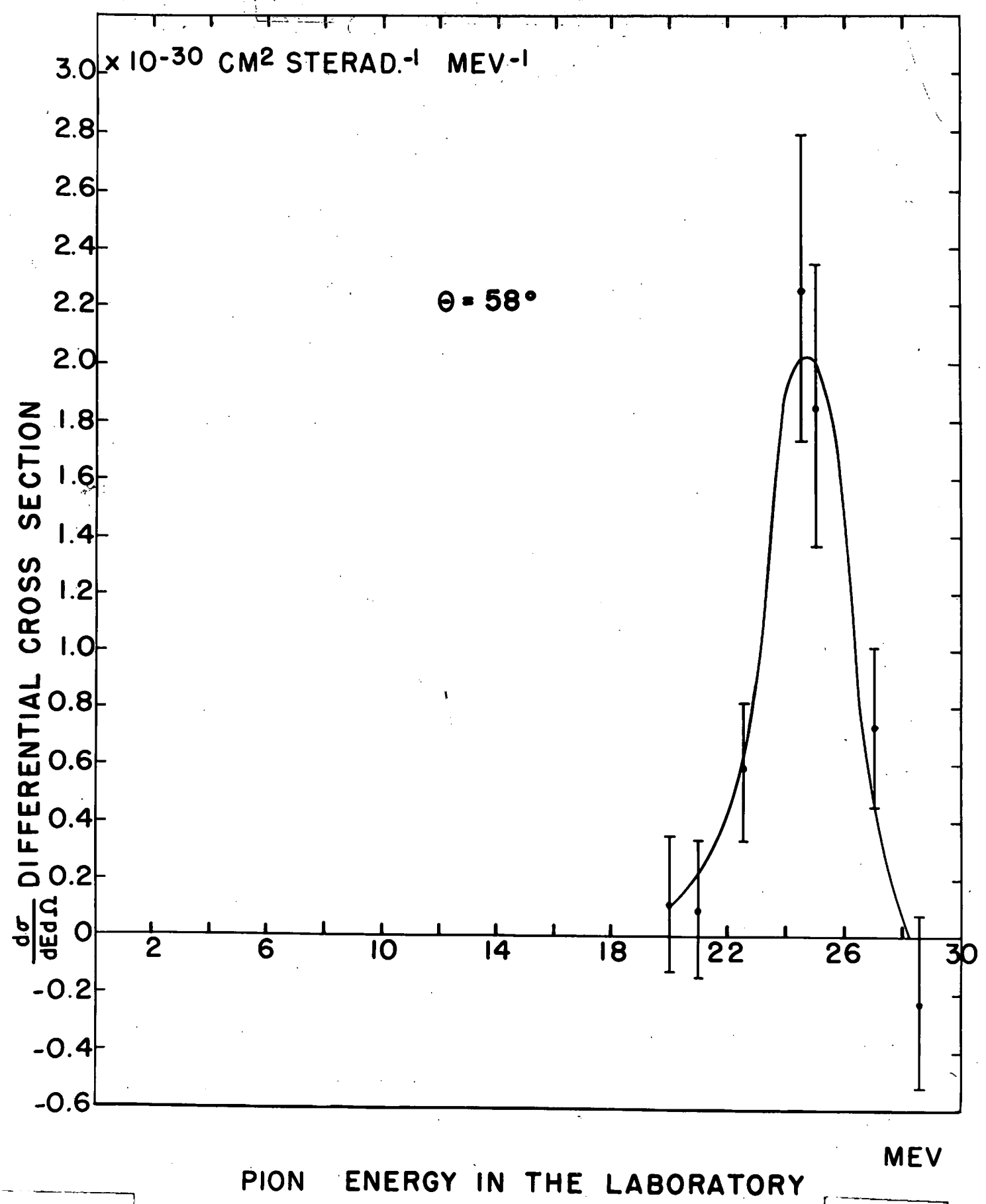
x 10-30 CM2 STERAD.-1 MEV-1
3.0
2.8
2.6
2.4
2.2
2.0
1.8
1.6
1.4
1.2
1.0
0.8
0.6
0.4
0.2
0
-0.2
-0.4
-0.6
θ = 58°
dσ/dEdΩ DIFFERENTIAL CROSS SECTION
2
6
10
14
18
22
26
30
MEV
PION ENERGY IN THE LABORATORY

FIG. 6

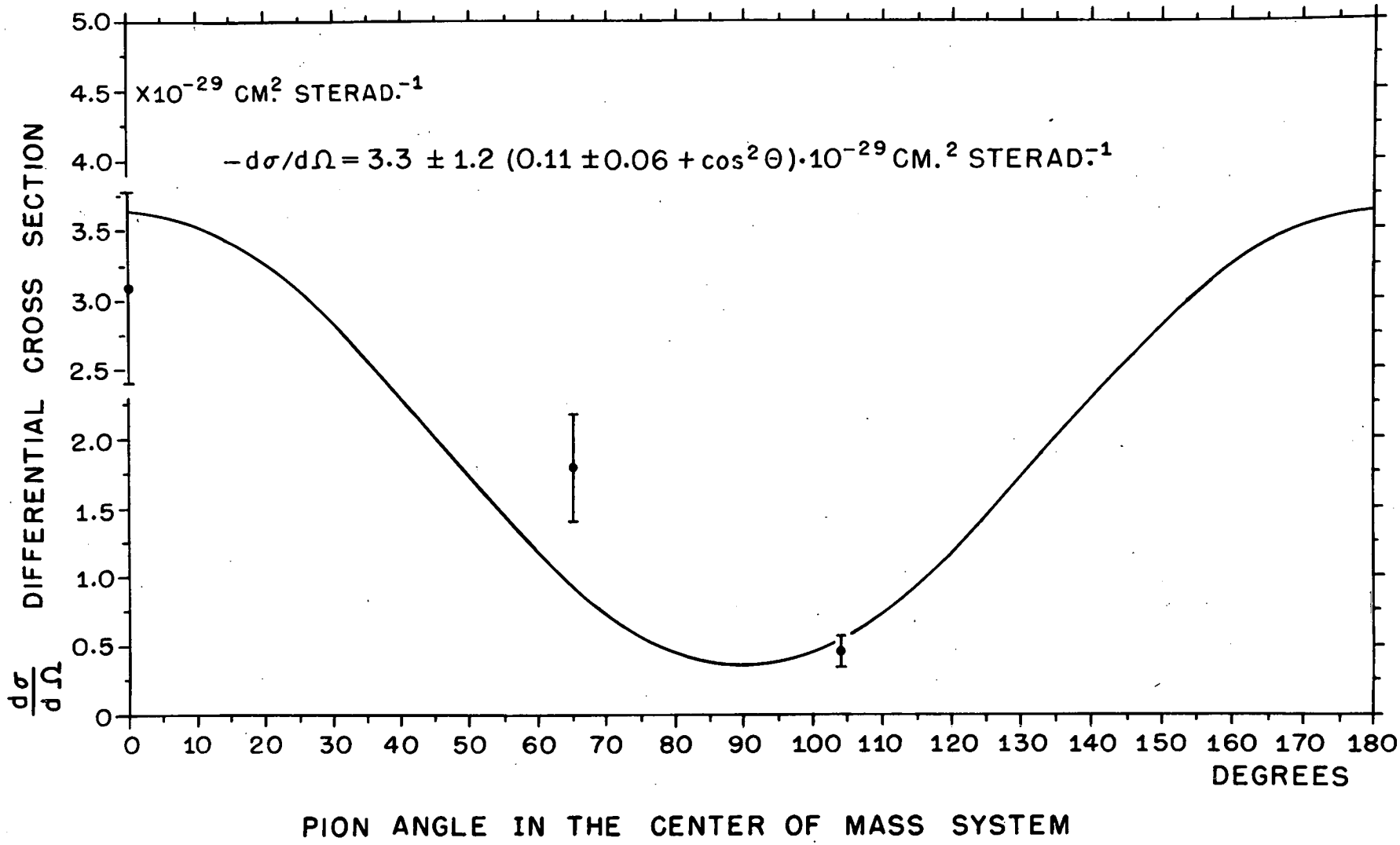
$\frac{d\sigma}{d\Omega}$ DIFFERENTIAL CROSS SECTION
X10^{-29} CM.^{2} STERAD.$^{-1}$
$-d\sigma/d\Omega = 3.3 \pm 1.2\ (0.11 \pm 0.06 + \cos^2\Theta)\cdot 10^{-29}$ CM.^{2} STERAD.$^{-1}$
5.0
4.5
4.0
3.5
3.0
2.5
2.0
1.5
1.0
0.5
0
0 10 20 30 40 50 60 70 80 90 100 110 120 130 140 150 160 170 180
DEGREES
PION ANGLE IN THE CENTER OF MASS SYSTEM

Fig. 7

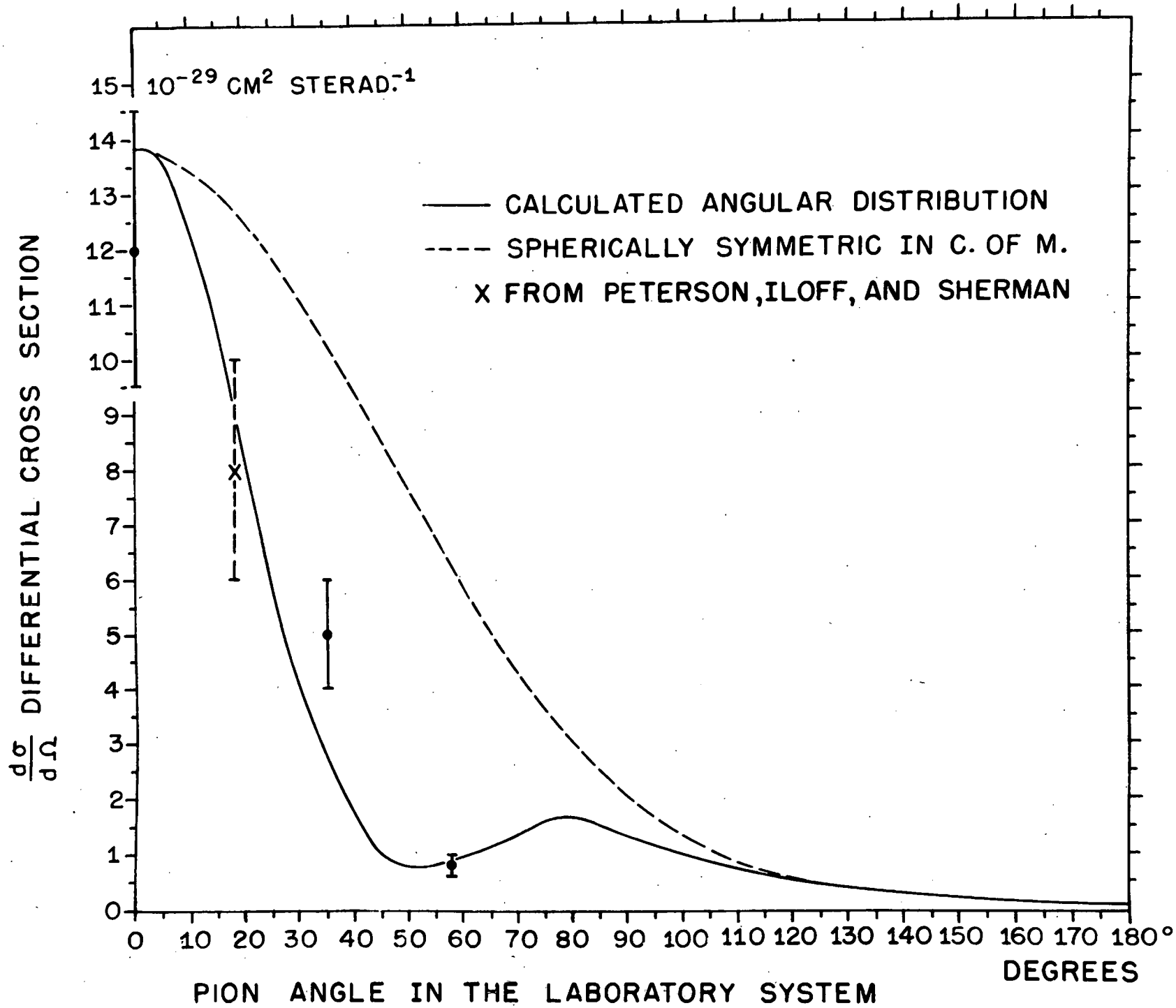
10^{-29} CM^2 STERAD.$^{-1}$
CALCULATED ANGULAR DISTRIBUTION
SPHERICALLY SYMMETRIC IN C. OF M.
X FROM PETERSON, ILOFF, AND SHERMAN
$\frac{d\sigma}{d\Omega}$ DIFFERENTIAL CROSS SECTION
0 1 2 3 4 5 6 7 8 9 10 11 12 13 14 15
0 10 20 30 40 50 60 70 80 90 100 110 120 130 140 150 160 170 180°
DEGREES
PION ANGLE IN THE LABORATORY SYSTEM

Fig. 8

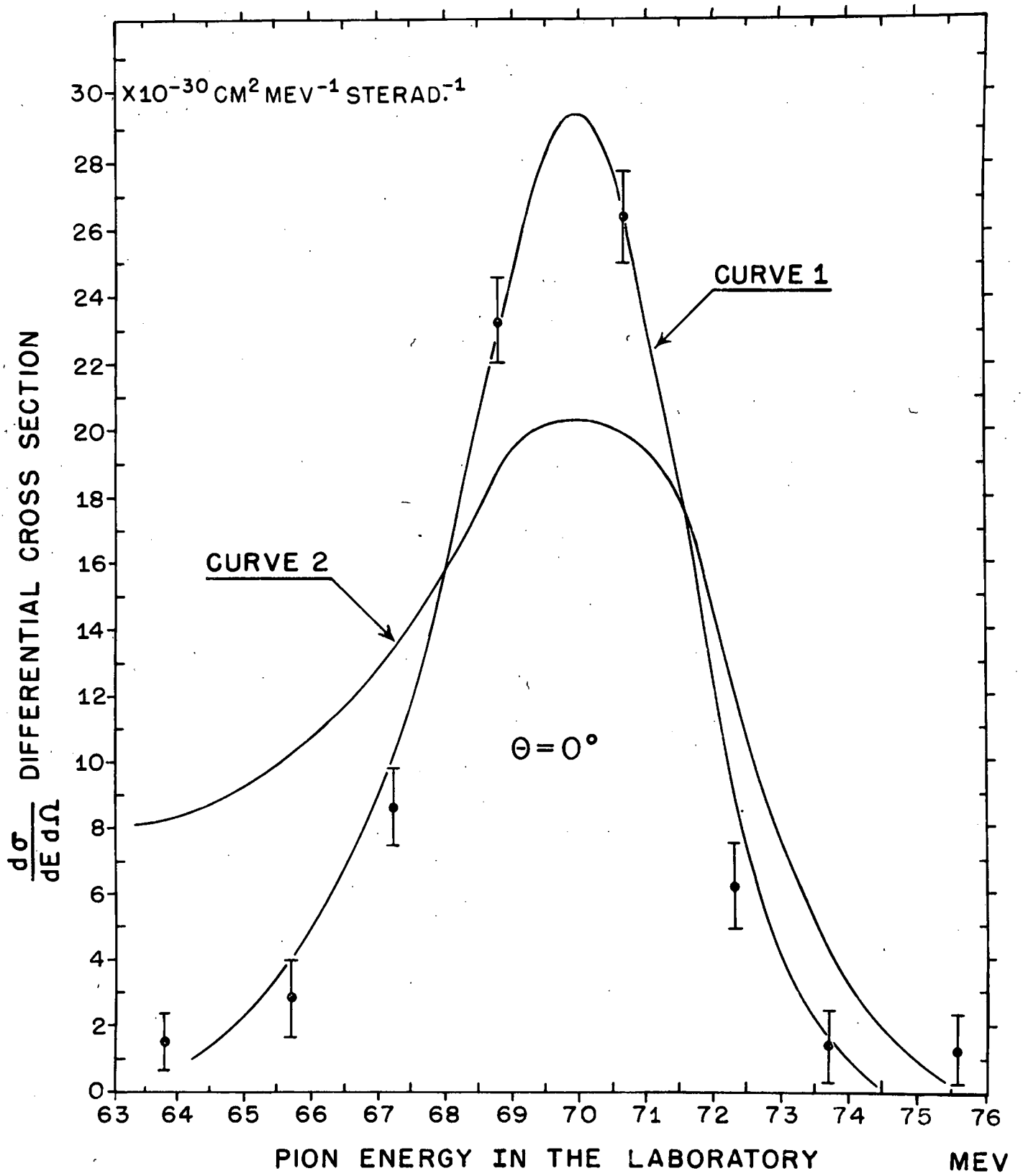
X10^{-30} CM^2 MEV^{-1} STERAD.$^{-1}$
$\frac{d\sigma}{dE\,d\Omega}$ DIFFERENTIAL CROSS SECTION
CURVE 1
CURVE 2
$\Theta = 0°$
PION ENERGY IN THE LABORATORY
MEV
0
2
4
6
8
10
12
14
16
18
20
22
24
26
28
30
63
64
65
66
67
68
69
70
71
72
73
74
75
76

FIG. 9

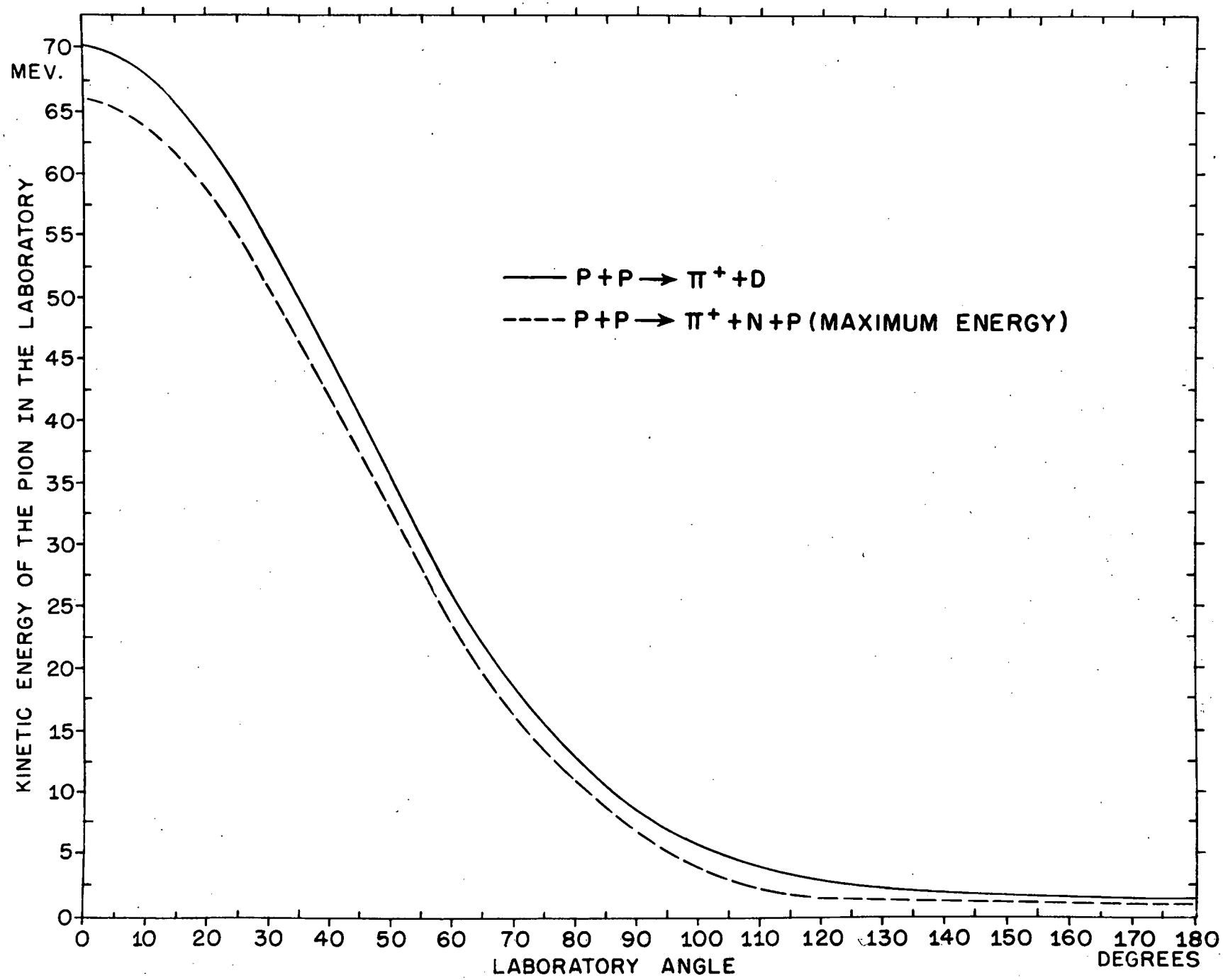
KINETIC ENERGY OF THE PION IN THE LABORATORY
MEV.
70
65
60
55
50
45
40
35
30
25
20
15
10
5
0
0 10 20 30 40 50 60 70 80 90 100 110 120 130 140 150 160 170 180
LABORATORY ANGLE
DEGREES
P + P → π⁺ + D
P + P → π⁺ + N + P (MAXIMUM ENERGY)

FIG. 10

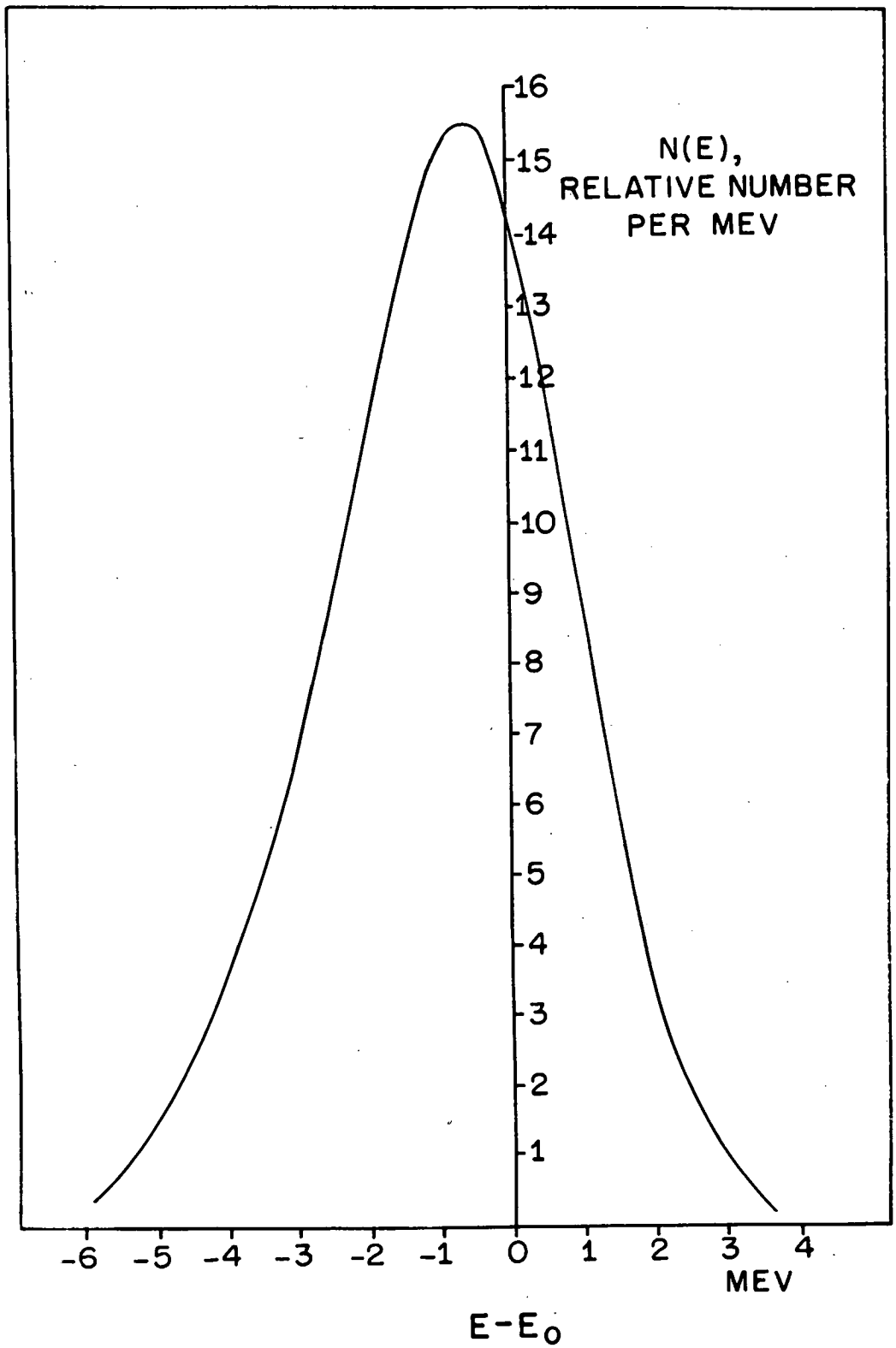
N(E),
RELATIVE NUMBER
PER MEV
16
15
14
13
12
11
10
9
8
7
6
5
4
3
2
1
-6
-5
-4
-3
-2
-1
0
1
2
3
4
MEV
E-E0

FIG. 11